

UC Berkeley

UC Berkeley Previously Published Works

Title

Role of Clays in the Enhanced Recovery of Petroleum From Some California Sands

Permalink

<https://escholarship.org/uc/item/66c4v9zv>

Journal

Journal of Petroleum Technology, 35(03)

ISSN

0149-2136

Authors

Somerton, WH
Radke, CJ

Publication Date

1983-03-01

DOI

10.2118/8845-pa

Peer reviewed

Role of Clays in the Enhanced Recovery of Petroleum From Some California Sands

W.H. Somerton, SPE, U. of California

C.J. Radke, SPE, U. of California

Summary

Many oil-producing formations contain significant amounts of clay. Because of the large surface area and the high reactivity of such surfaces, the response of the formations to various recovery processes may be dominated by the reactions of the clays. Thus, the success or failure of enhanced oil recovery (EOR) methods may be controlled to a large extent by the amount and type of clays in the formations to which the methods are being applied.

This paper evaluates the type and amounts of clays and clay minerals present in typical oil-producing formations that may be candidates for application of EOR methods. After identification of the clay minerals present, tests are run on the extracted clay fractions to determine cationexchange capacities (CEC's), surface areas, and chemical-loss characteristics. Flood tests are run on core samples to evaluate the magnitude of chemical loss and to note the change in flow characteristics while different fluids, which might be used in EOR operations, are flowed through the core. This background material is used to test predictive equations developed for screening reservoirs for EOR applications and for optimizing process variables. Techniques to counter the effects of rockfluid interactions are considered.

Introduction

Because of the large effective surface areas of clays contained in oil reservoir formations and because of the high degree of reactivity of such surfaces, clays may play a disproportionate role in the success or failure of EOR techniques. Clays adsorb many substances that may be 0149-2136/83/0003-8845\$00.25 Copyright 1983 Society of Petroleum Engineers of AI ME MARCH 1983 injected into the reservoir to improve oil recovery. In many cases, surfactants and polymers adsorb on clay surfaces in sufficient amounts to make the recovery process uneconomical. The ion-exchange capacity of clay minerals may have two detrimental effects: (1) release of divalent ions can cause surfactant precipitation, increased surfactant oil solubility, loss of ultralow interfacial tension, and polymer degradation; (2) ionexchange reactions with concomitant surface-charge effects may cause structural damage to the formation. Clay swelling and migration of fines also may result from causes other than changes in the system chemistry. For example, rate effects are important in fines migration. Rapid changes in flow rate, salinity, or temperature may cause plugging, whereas only negligible plugging may result if the rates of change are decreased.¹

Many oil reservoir formations contain substantial amounts of fines including considerable amounts of clay minerals. Screening tests must be conducted on object formations to provide information on potential problems and to suggest means of minimizing their effects. There also are possibilities that certain clay mineral components can be used advantageously in mobility control. This is particularly important in heterogeneous formations containing viscous residual oils.

Test Program

The overall objectives of this research program are to evaluate the effects that clays present in typical oilproducing formations have on the failure or success of EOR operations. Methods of dealing with the detrimental effects of clays and enhancing the favorable characteristics of clays, if any, are explored. The first phase of the project is limited to chemical methods of EOR.

TABLE 1—X-RAY MINERAL ANALYSES OF VARIOUS OIL SANDS (%)

Well Sample	Size (μm)	Montmorillonite	Kaolinite	Mica	Calcite	Zeolite	Quartz	Feldspar	Others*
Wilmington composite	< 2	45	3	10	—	7	6	10	19
	< 43	4	2	10	—	12	25	40	7
	all	—	—	2	—	—	40	55	3
B110 9,931 ft	< 2	50	8	15	10	2	3	5	7
	< 43	12	13	12	3	5	15	40	10
	all	12	8	20	10	4	10	20	16
B110 4,914 ft	< 2	15	2	7	—	6	15	45	10
	< 43	5	3	10	—	2	12	62	6
	all	—	—	5	—	—	30	63	2
Huntington 4,894 ft	< 2	65	6	10	—	—	8	10	1
	< 43	10	5	7	—	—	15	60	2
	all	6	—	7	—	—	40	45	3
4,897 ft	< 2	65	3	10	—	—	12	10	—
	< 43	8	3	6	—	—	15	65	3
	all	—	—	6	3	—	45	45	1
Coalinga	< 2	50	20	—	—	12	8	8	2
	< 43	4	3	—	—	45	25	20	3
	all	2	2	—	—	15	45	35	1

*Determined by difference.

Core samples are collected from oil-producing formations considered possible candidates for the application of EOR methods. These cores are cataloged as to geologic age, zone, depth, and general petrographic description. After the cores are extracted with organic solvents, they are

subjected to grain-size and surface area analyses. The overall mineral composition of the fines fraction is determined.

Core packs of the extracted sand are used to study the effects of various injection fluids on the flow behavior of the pack. Analysis of the effluent from these flow tests is used to monitor changes in the physical and chemical characteristics of the system. Column tests run in a companion project² provide additional data on chemical/rock interactions.

Test Sample Selection and Description

Core samples have been collected from zones where alkaline water flooding trials are planned-i.e., Ranger zone of the Wilmington field and Main zone of the Huntington Beach offshore field-and from the Temblor 2 zone of the East Coalinga field where a polymer flood was attempted.

Wilmington field core samples were taken from Well B11D in Fault Block 7 from the Ranger zone (Repetta formation, Lower Pliocene). This unconsolidated sand sample is gray to greenish gray in color and is sorted poorly to moderately. In thin-section the sample is seen to consist of quartz, feldspars (plagioclase and Kfeldspar), volcanic rock fragments, biotite, and accessory minerals in approximate amounts as shown in Table 1. The accessory minerals include garnet, sphene, epidote, and hornblende. The quartz grains are monocrystalline exhibiting undulatory extinction, ranging from rounded to subangular in shape, in contrast to the other mineral grains, which are sub angular to angular. This sand is immature both texturally and compositionally, and appears to have a plutonic and volcanic source area. The diagenetic alterations that have taken place in the rock appear to be chloritization of biotite and possibly the alteration of some feldspars and volcanic rock fragments into clay. This does not exclude the possibility of the primary depositional origin of the clays.

A composite Ranger zone sample was prepared from several different cores to give a typical composition for comparative tests by several different laboratories. Cores from other wells, zones, and fields are described in the same manner as in the preceding paragraph.

Petrographic/Mineralogical Analyses

Grain Size Analysis

Test specimens were selected from the center of the 8.9-cm diameter cores to minimize the possibility of contamination with drilling fluid. Since the test specimens contained residual reservoir fluids, they were extracted with toluene in a Soxhlet extraction apparatus and dried in a vacuum oven at about 60 °C.

The extracted sample for grain-size analysis was wet-sieved through a 325-mesh (43- μ m) screen. The coarser fraction was vacuum-oven dried and was then dry-sieved through a set of Tyler screens. Dry material that passed the 325-mesh (43- μ m) screen was added to the wet-sieve fine fraction and the

total was reported as weight percent finer than 43 μm in Table 2. Size distribution of the fines fraction then was determined by an optical particle-size analyzer. Results of the size analysis were plotted on the conventional cumulative-distribution plot, and the median grain size (d_{50}) and the size distribution function (d_{90}/d_{10}) were determined. This latter number is unity for a single grain size and decreases as the size distribution becomes broader. These values and the finer than 4- μm wt% are given in Table 2.

Table 2 shows the results of grain-size analysis run on eight test specimens of the Ranger-zone core. "Treatment" refers to whether the specimen was new (unflooded) or whether it had been subjected to caustic flooding as reported in the companion project.² The purpose was to determine whether fines had been lost in the flooding process or whether some alteration of the mineral structure could be detected. The results showed a large range of values. The percentage of fines ranged from 11.6 to 39.9% and the clay fraction ranged from 1.2 to 6.0% of the total. Note that the treated samples generally show larger amounts of both fines and clay fractions than the untreated samples. This is probably a sampling problem and is not associated with chemical reactions. There is evidence that caustic does release fines from larger mineral grain surfaces, but the amounts are probably small compared to the quantities just mentioned.

TABLE 2—GRAIN-SIZE ANALYSES OF SANDS

Source	Depth (ft)	Treatment	< 43 μm (wt%)	< 4 μm (wt%)	< 2 μm	d_{50} (μm)	d_{90}/d_{10}
Wilmington (Ranger)	4,931	none	18.8	1.7	—	105	0.078
	4,931	NaOH	24.6	4.4	—	190	0.101
	4,932	NaOH	32.6	4.1	—	115	0.025
	4,933	none	11.6	1.3	—	200	0.024
	4,934	none	26.6	4.0	—	135	0.015
	4,934	NaOH	39.9	6.0	—	100	0.153
	4,913	none	28.7	—	2.3	—	—
	4,914	none	25.7	—	1.8	—	—
	composite	none	27.5	3.5	2.6	107	0.034
Huntington Beach	4,894	none	14.5	2.6	1.3	160	0.027
	4,897	none	9.4	—	0.8	—	—
Coalinga		none	12.5	—	0.9	—	—

The median grain size and the size-distribution function give a qualitative measure of the surface area of the sample. For common geometries (i.e., spheres, cubes, and disks) the surface area per unit volume increases by an order of magnitude for every order of magnitude decrease in grain diameter. Surface areas also can be estimated from the median grain diameter and the sizedistribution function. The latter value is important in that the lower its numerical magnitude, the greater is the amount of fines, relative to the median grain diameter. Surface areas estimated from grain-size analyses give very low values for formations containing clays. This is because of the platy nature of the minerals included in this group. It is possible to apply a

modified shape factor based on the clay mineral content. Surface areas derived by these means may be more useful for surface reactions involving large molecules (e.g., polymers, surfactants) than those obtained from BET analysis, which measures all the surfaces that may be contacted by small molecules, comparable in size to nitrogen.

There is no general agreement as to the definition of clay fraction based on grain size. Four micrometers commonly is considered to be the limiting size. Although clay minerals can be larger than 4 μm , concentration of clay minerals will increase as the grain size decreases. X-ray analysis indicated that 2 μm is probably a better upper limit. This is because the quartz and feldspar contents are reduced substantially, thus permitting a much better determination of clay minerals. The < 2- μm material is separated by a sedimentation process. Since this method is based on the application of Stokes' law and assumes spherical grains, platy minerals substantially larger than 2 μm in two dimensions will appear in the separated material. This is confirmed by scanning electron-microscope (SEM) studies reported later.

The grain-size analysis procedure was changed later to eliminate the sieve separation of the > 43- μm material and the size analysis of the < 43- μm material using the optical particle-size analyzer. The finer-than-43- μm material was separated by wet- and dry-sieving and the < 2- μm material was separated by the sedimentation method. Table 2 shows the results of size analysis on a variety of core materials using this latter technique. The Wilmington core material contains much more fines and clay fractions than the Huntington Beach or Coalinga cores. The < 2- μm material reported here was used in all subsequent clay mineral identification tests.

X-Ray Analysis

Test specimens for clay minerals identification by X-ray analysis were prepared by suspending a portion of the fines (< 43 μm) from the grain-size analysis in distilled water containing a small amount of sodium hexametaphosphate and placing the mixture in an ultrasonic bath to disperse the clays. The mixture then was placed in a sedimentation column for a length of time sufficient to allow the > 2- μm material to settle out. The liquid containing the clay fraction was centrifuged and smear mounts were prepared and air-dried for X-ray analysis.

X-ray analyses also were run on the total core material and the < 43- μm fraction. The total sample was run to give the overall mineral composition of the core, the < 2- μm fraction was run to give good definition of the clay minerals present in the core.

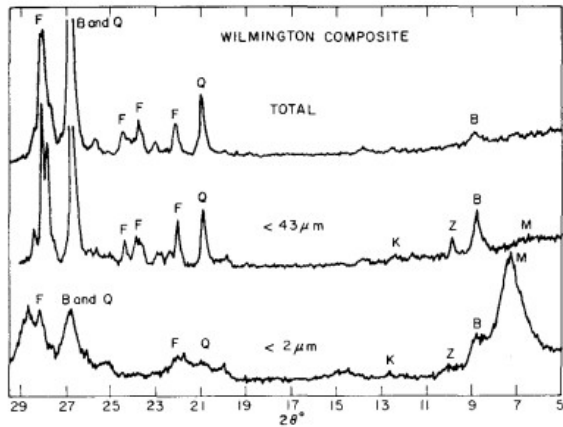


Fig. 1—X-ray diffraction patterns for Wilmington composite sand.

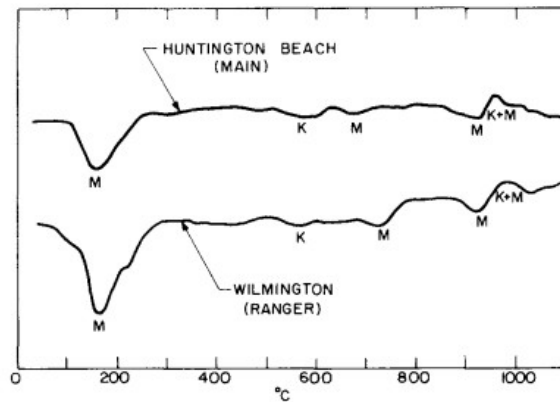


Fig. 2—Differential thermal analysis records for Wilmington and Huntington Beach sands.

Results of X-ray analyses are given in Table 1. The dominant clay mineral in these oil sands is montmorillonite with a smaller amount of kaolinite present in most cases. Tests on glycolated specimens confirmed that the montmorillonite was an expandable clay mineral. Illite or mixed-layer clay minerals could not be identified specifically, although some of the mica reported in the analyses could be attributed to small amounts of these clay types. Quartz and feldspars were the other dominant minerals in most cases. Both plagioclase and K-feldspar were present in all samples but are not reported separately. A zeolite was present in several samples and in a surprisingly large amount in the Coalinga fines. Calcite was present in one core sample and was identified tentatively in another. The balance of mineral content is reported in the last column as other minerals and amorphous materials.

As expected, the clay-mineral content was concentrated in the $< 2\text{-}\mu\text{m}$ fraction. This is demonstrated clearly in Fig. 1, which shows the X-ray-diffraction patterns for all three size groupings for Wilmington composite sand. The large montmorillonite peak for the $< 2\text{-}\mu\text{m}$ fraction essentially disappears for the $< 43\text{-}\mu\text{m}$ fraction and the total sand sample. The principal peaks for the major minerals are identified on the patterns by appropriate letters. In addition to the clay minerals present in the $< 2\text{-}\mu\text{m}$ fraction, significant amounts of quartz and feldspars also occur. This is important because of the large surface areas of minerals in the clay fraction making large contributions to chemical reactions that may occur.

The presence of the zeolite mineral, clinoptilolite, was confirmed by R. L. Hay.³ Zeolites are hydrous aluminosilicates that are alteration products of volcanic materials. Clinoptilolite has a Si/Al ratio between 4.25 and 5.0. The net negative charge in the tetrahedra framework is balanced predominantly by Na and K ions. This mineral commonly occurs together with montmorillonite and is found in Miocene formations in the central coast

ranges of California.⁴ The importance of the presence of zeolites is their open structure and their large cation exchange capacities (CEC's).

Differential Thermal Analysis

Differential thermal analysis (DTA) tests were run on one Wilmington Ranger zone sample and one Huntington Beach Main zone sample. It was necessary to treat the $< 2\text{-}\mu\text{m}$ fraction with hydrogen peroxide to remove organics before running the DTA. Fig. 2 shows the results for the two peroxide-treated samples. Although a quantitative interpretation of these results was not attempted, it is apparent that substantial amounts of montmorillonite and smaller amounts of kaolinite are present in both samples. Again, no illite or mixed-layer clay minerals could be identified.

SEM Analysis

SEM photographs were taken of the $< 2\text{-}\mu\text{m}$ material as a further aid in mineral identification. This technique, when used in conjunction with the energy-dispersive analysis of X-rays (EDAX) attachment, gives a bulk chemical analysis of the minerals. The $< 2\text{-}\mu\text{m}$ material was separated by sedimentation as for X-ray analysis samples, except that the centrifuged material was freeze-dried to disperse the mineral grains and to avoid caking. The best SEM photographs were obtained by applying a thin coat of carbon followed by a thin coat of gold to the test specimen. The SEM photographs and corresponding EDAX records for several common minerals separated from Wilmington oil sands are shown in Fig. 3.

Fig. 3a shows the crushed quartz grains with the black bar at the bottom of the photograph used to represent a length of $10\ \mu\text{m}$. The EDAX scan shows only the Si peak along with some minor background. Fig. 3b shows crushed K-feldspar and the EDAX record indicating Al to the left of the Si peak and K to the right, again with some minor background. Fig. 3c is for montmorillonite at a $2\text{-}\mu\text{m}$ scale. The EDAX record shows the presence of Al, Si, K, Ca, Ti, and Fe, respectively, from left to right. Fig. 3d is biotite, which appears to be slightly overcoated. The EDAX record for biotite shows the presence of Mg, Al, Si, K, Ti, and Fe, again from left to right.

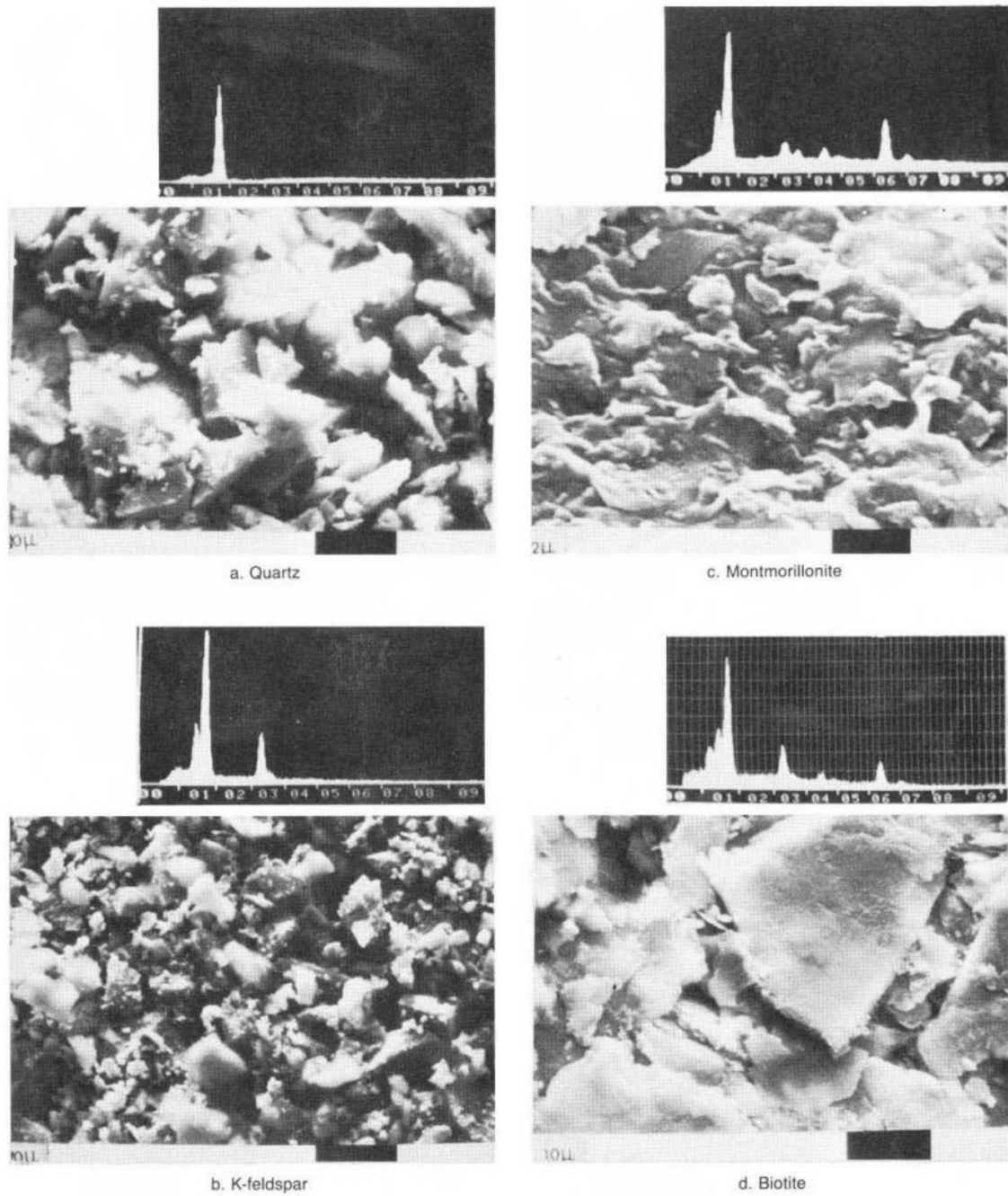
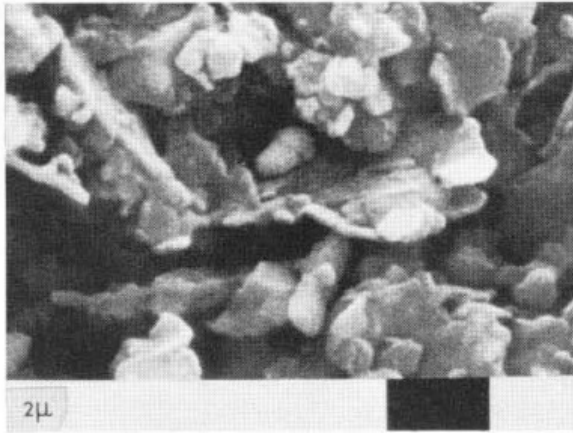
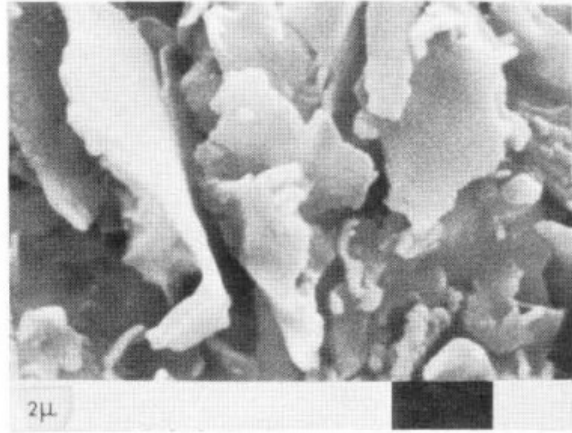


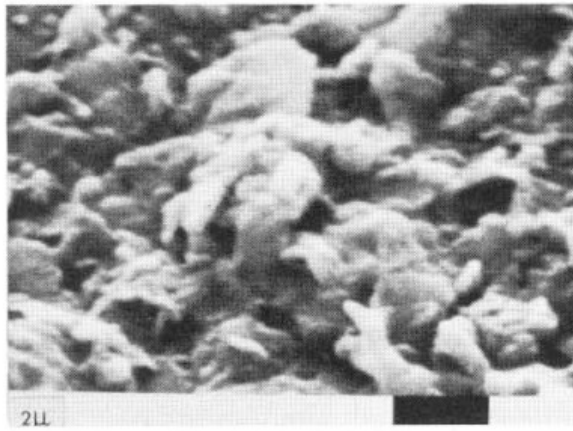
Fig. 3—SEM photographs and EDAX scans for various minerals.



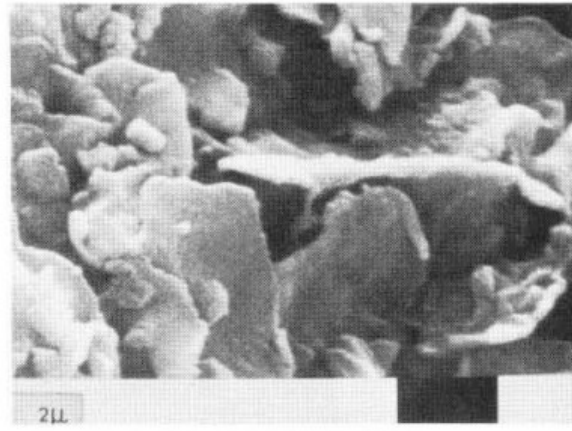
a. Wilmington Composite



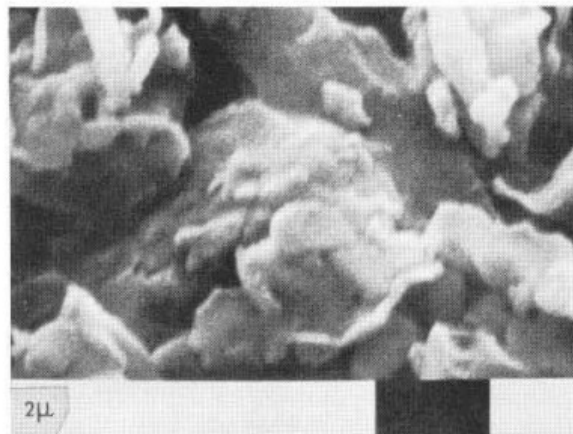
d. Huntington Beach 4894



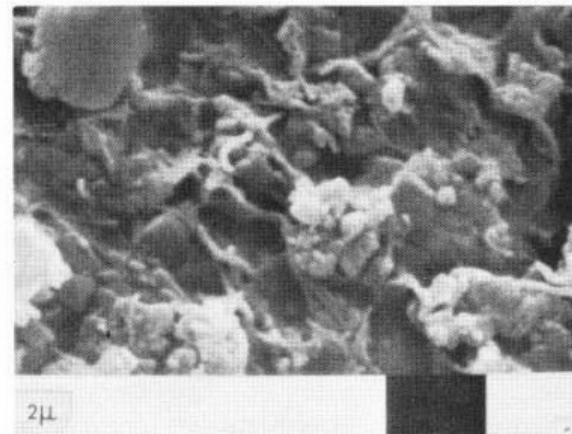
b. Wilmington B110 4913



e. Huntington Beach 4897



c. Wilmington B110 4914



f. Coalinga

Fig. 4—SEM photographs of oil sands.

**TABLE 3—FLUID-FLOW TEST RESULTS FOR WILMINGTON
COMPOSITE SAND**

Fluid Flowing	Initial Permeability (md)	Flowing Fluid (PV)	Final Permeability (md)
Nitrogen	185	—	—
Sim. Brine	145	4	92
Conc. NaCl	92	5	74
1.0 wt% NaCl	74	3	44
1.0 wt% NaOH	44	3	36
+ 1.0 wt% NaCl	—	3 to 6	variable (37 to 43)
Polymer	variable	5	23

TABLE 4—CALCIUM CATIONIC-EXCHANGE CAPACITIES

Sample	Z _r (meq/100 g)	Montmorillonite (wt%)
Wilmington		
composite	2.0 ± 0.9	1.2
B110 at 4,913 ft	2.4 ± 1.3	1.5
B110 at 4,914 ft	0.9 ± 0.8	0.27
Huntington		
4,894 ft	1.3 ± 0.5	0.85
4,897 ft	1.3 ± 0.5	0.52
Coalinga	0.9 ± 0.5	0.45

Fig. 4 shows SEM photographs for the six oil sands used in this study. The scale for all six photographs is 2 μm , and < 2- μm sedimented material was used in all cases.

Although SEM with the EDAX attachment is useful in identifying specific minerals, it is of limited use for quantitative analysis. It is extremely useful in identifying minor constituents having unique chemical compositions. For example, the presence of sulfate was observed in the effluent from a caustic flooding test and the presence of gypsum in the core was suspected. An EDAX scan for sulfur in the Wilmington Ranger zone sand showed the presence of sulfur, but it was always associated with montmorillonite. We tentatively concluded that the sulfur detected in the scan was associated with the residual organic material that was detected on the extracted sand during the initial DT A tests.

Fluid-Flow Tests

Tests to evaluate fluid-flow characteristics for different fluids that might be flowed through the reservoir rock in EOR operations were run on the Wilmington composite sand. The extracted core material was packed into a flow tube to a porosity close to that in the reservoir (31 %) and an air

permeability of 0.185 md. The core was vacuum saturated with simulated reservoir brine that contained both Ca and Mg ions. Several PV's of the brine was flowed through the core at a constant rate of about 0.3 md. Flow was continued until the pressure (and thus the permeability) were fully stabilized. The same procedure was repeated with a NaCl solution having the same salinity as the total salinity of the simulated brine (2.86 wt%), followed by a 1-wt% NaCl solution, a 1-wt% NaOH and 1-wt% NaCl solution, and a polymer solution containing the same concentration of NaOH and NaCl. Note that all these flow tests were run at reservoir temperature (52°C).

Table 3 is a summary of the flow-test results. It shows the initial permeability at the start of the test, the PV of fluid flowing to reach a stabilized permeability, and the final permeability. Note that at least an additional 2 PV was flowed through the core to confirm stability of permeability. Each time a new fluid was introduced into the core, a reduction in permeability occurred. This was consistent with Mungan's ¹ work and is similar to results reported by Muecke.⁵ Although no fines could be observed in the effluent, the permeability reduction must be attributed to a combination of clay swelling and migration of fines.

Chemical Interactions With Rock

Ref. 2 reports results of tests performed to determine EOR chemicals' interaction with formation rocks. Tests have been run primarily on toluene-extracted Wilmington oil sands reported in Table 2. A summary of this work follows.

Divalent Cation Exchange with Rock

Because chemical additives, such as surfactants and polymers, are sensitive to multivalent cations, exchange of hardness ions with reservoir rock is critically important to EOR processes.⁶⁻¹² CEC's and isotherms of selected California sands are being studied using both column tests and static jar tests. Column tests, which use the technique of frontal analysis, generally are accurate^{2,13,14} and perhaps more representative of field application. However, column testing requires extensive chemical analysis and, hence, is time consuming. Conversely, static tests suffer from lack of precision, especially when mineral grain sizes are large. Nevertheless, they are rapid and are replicated easily.

Table 4 gives the calcium CEC's for the six California oil sands at ambient temperature by the static method. Also shown are the weight percentages of montmorillonite in these sands. These data are obtained for the grain-size fraction < 43- μ m and are reported for the whole rock, assuming negligible capacity for the larger particle sizes. Two features are apparent from Table 4. First, noticeable error in the exchange capacities results from the concentration-difference measurements required in the static technique. Second, the exchange capacities generally parallel the montmorillonite content of the sands. This is expected from the large surface areas of clay

minerals and, in particular, from the large exchange capacity of montmorillonite-i. e., 100 meq/100 g.¹⁵

More important than the exchange capacity is the exchange isotherm. The ease with which hardness ions may be removed from reservoir rock by soft, saline preflushing depends primarily on the slope of the exchange isotherm^{16,17}; high isotherm slopes lead to inefficient hardness removal, and large preflush PV's are required even in the swept zones. Fig. 5 shows the calcium/sodium exchange isotherm for Wilmington sand at 52°C from frontal-analysis column testing. Isotherms for two salinities are reported and typical error bars are shown. The symbol $Z_{Ca^{++}}$ denotes the amount of calcium adsorbed on the rock in units of the exchange capacity. The two closed circles refer to static jar tests at ambient temperature and at the lower salinity. Agreement with the column results is adequate and confirms the insensitivity of calcium/sodium exchange to temperature.¹⁸ Note that the CEC in Fig. 5 is larger than those reported in Table 4 by static testing. On repeating the column experiment with the same rock sample, we find that the isotherms are reversible, but they drift to a higher and more stable calcium uptake, as shown in Fig. 5. Apparently, repetitive and prolonged column flushing with sodium chloride exposes additional exchange sites.

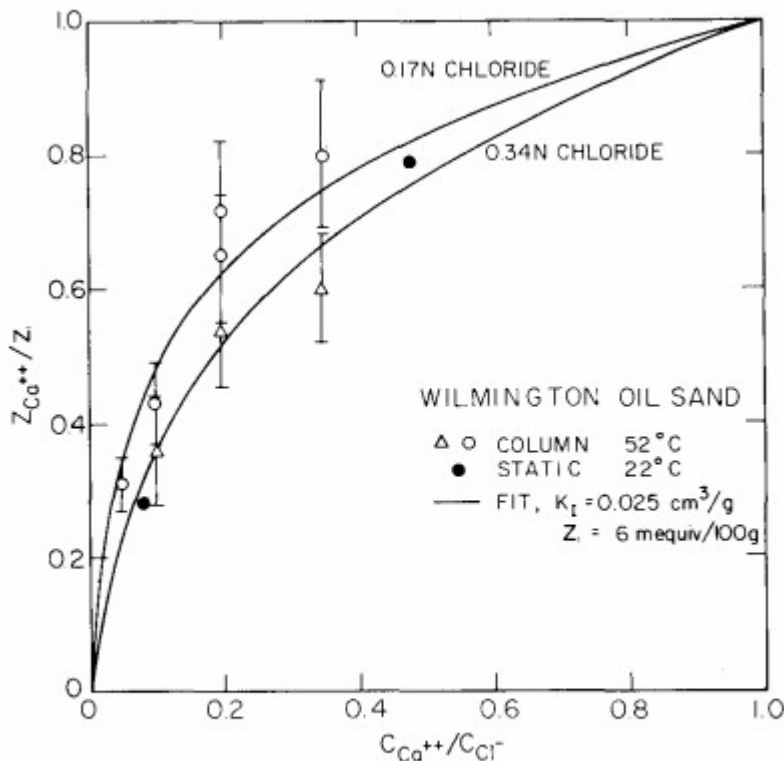


Fig. 5—Calcium/sodium-exchange isotherm for Wilmington and Huntington Beach sands.

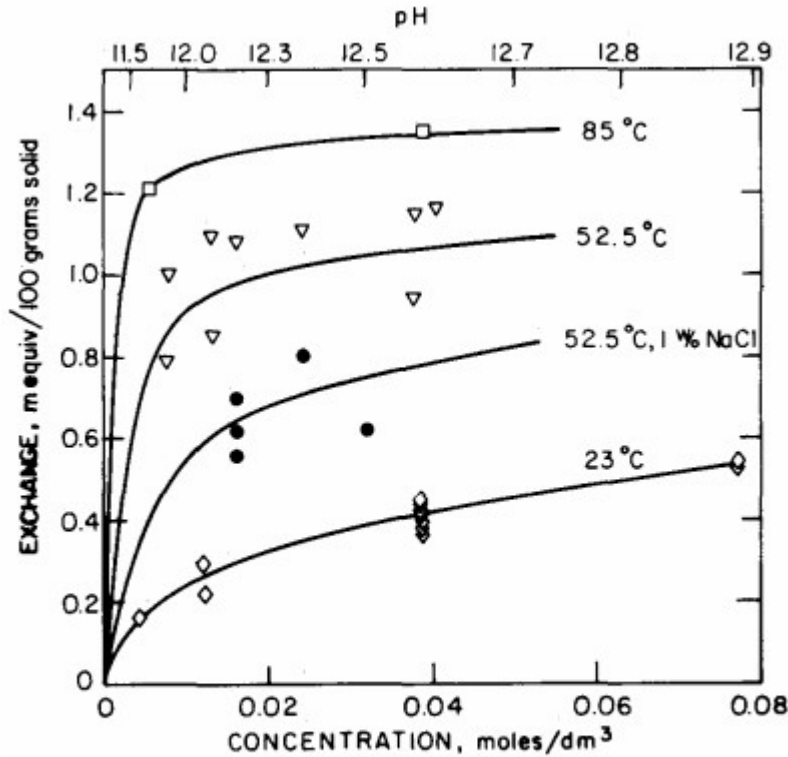


Fig. 6—Hydroxide-exchange isotherms for Wilmington oil sand at three temperatures and two salinities.

The solid lines in Fig. 5 are a fit to the mass-action equation (i.e., for the exchange $M_2Ca + 2NaCl = 2MNa + CaCl_2$, where M denotes a mineral-base exchange site),

$$\frac{C_{Cl^-}}{Z_t} K_I = \frac{(1 - Z_{Ca^{++}}/Z_t)^2 (C_{Ca^{++}}/C_{Cl^-})}{(1 - C_{Ca^{++}}/C_{Cl^-})^2 (Z_{Ca^{++}}/Z_t)}, \dots (1)$$

where C denotes a solution concentration in equivalent units, Z_t is the calcium CEC, and K_I is the ion-exchange equilibrium constant. For the Wilmington sand, Eq. 1 correctly portrays the ionic-strength effect that higher salinities lead to smaller uptake of calcium and, hence, more efficient removal. Use of calcium/sodium exchange isotherms in chemical flood simulators has been discussed.^{7,8,10,19,20} Particularly for the Wilmington sand, the isotherm of Fig. 5 predicts that a large number of PV's of sodium chloride preflush will be required to remove effectively the reservoir hardness ions.²

Alkali Exchange with Rocks

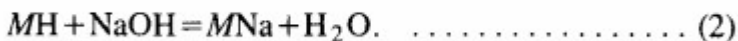
In alkaline waterflooding²¹ and in alkali preflushing or alkaline surfactant flooding,^{11,12} interaction of hydroxide with reservoir sands is a critical, if not dominant, factor. Interaction of alkali with rock minerals is complicated, and can include surface exchange and hydrolysis,^{2,22} congruent and incongruent

dissolution reactions,^{2,23} and insoluble salt formation by reaction with hardness ions in the pore fluids and exchanged from the rock surfaces.^{2,11,24} These interactions may be classified further into reversible or irreversible, and kinetic-controlled or instantaneous. This section briefly discusses the reversible ion exchange of caustic with reservoir sand, a contribution normally not considered, but which controls the advance rate of alkali in a reservoir.

Caustic exchange with rock was studied by frontal analysis chromatography, as discussed in the previous section. Short columns and high flow rates are used to lessen any contribution from dissolution reactions. Effluent hydroxide concentrations are determined by potentiometric titration. If glass electrodes are used, the pH values must be converted to concentrations to accomplish the material balances required in the frontal analysis technique. Otherwise, alkali uptake is underestimated.^{25,26}

Fig. 6 gives the adsorption or exchange of hydroxide on sodium-exchanged Wilmington sand at two salinities and three temperatures.²⁶ The concentration and pH scales refer to room temperature. The hydroxide adsorption is approximately Langmuirian, and increases with increasing temperature, but decreases with increasing salt. We stress that the isotherms in Fig. 6 are reversible, as are those for calcium/sodium exchange in Fig. 5. Cyclical scrubbing of the column with brine followed by reinjection of caustic always gives the same adsorption isotherm.

The hydroxide isotherms in Fig. 6 may be explained qualitatively by sodium/hydrogen/weak-acid exchange with the reservoir rock as



Sodium/hydrogen ion exchange does not follow the same functionality as that for sodium/calcium exchange in Eq. 1. Based on the concept of ionizable surface acid groups, MH, and Eq. 2, Bunge argues that sodium/hydrogen ion exchange would quantitatively obey a Langmuir isotherm.²⁷ Likewise Bunge²⁷ demonstrates that the mass-action equilibrium of Eq. 2 can reflect increased hydroxyl uptake at higher temperatures and decreased hydroxyl uptake at higher salinities, as found in Fig. 6.

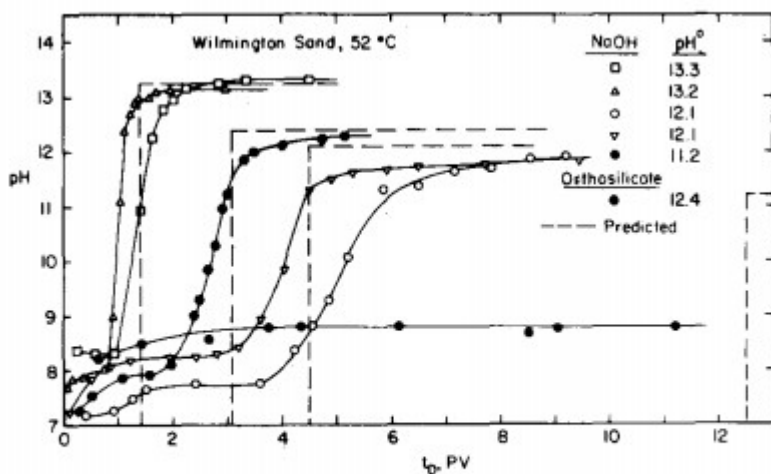


Fig. 7—Hydroxide concentration histories for tertiary oil floods in Wilmington oil sands.

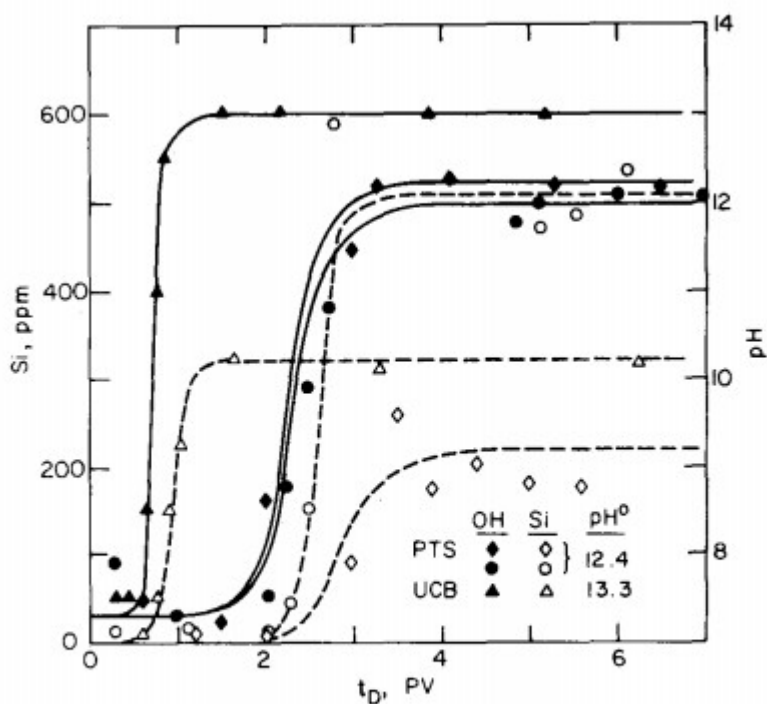


Fig. 8—Concentration histories of hydroxide and silicate for Wilmington oil sand; lines are eye-fit.

Although the hydroxide-exchange amounts in Fig. 6 are less than those for calcium/sodium exchange in Table 4, they nevertheless greatly retard the advance rate of alkali in a reservoir. Fig. 7 shows the elution of hydroxide from tertiary oil floods in the Wilmington sand for several injected pH values, all in 1-wt% sodium chloride. As the injected pH is lowered, the alkali takes

progressively longer to elute from the core. With an injected inlet pH of 11.2, hydroxide does not appear in the effluent even after 10 PV of flooding. The dashed lines in Fig. 7 are predicted *a priori* using standard equilibrium chromatography theory and the appropriate exchange isotherm (i.e., 52°C and 1-wt% sodium chloride) in Fig. 6.^{16,17,26} Even though dispersion distorts the hydroxide-concentration histories, the mean elution times are well-represented by the simple equilibrium ion-exchange theory. Again, it is the isotherm slopes or chords that control concentration velocities, with higher pH values having smaller slopes; hence, they yield quicker elution times. Elution of the sodium orthosilicate (i.e., a molar ratio of Na₂O/SiO₂ of 2: 1) is predicted successfully by the caustic-exchange isotherm of Fig. 6 showing that orthosilicate has mineral-exchange properties identical to those of caustic, when compared at equivalent alkalinities. If chromatographic lag is to be avoided in a field application of alkali, Fig. 7 clearly shows that higher pH values should be considered.

Alkali Reaction with Rock

In addition to ion-exchange reactions with rock surfaces, alkali can react directly with specific rock minerals. A well-documented example is the incongruent dissolution of anhydrite and gypsum in alkali to produce the lesssoluble calcium hydroxide-i.e., $\text{CaSO}_4(\text{s}) + 2\text{NaOH} = \text{Ca}(\text{OH})_2(\text{s}) + \text{Na}_2\text{SO}_4$.^{11,22} A second, less understood reaction, is that of dissolving alkali with reservoir rock to yield soluble silica. Although soluble silica has been observed after contacting reservoir rock with alkali,¹ the reaction is considered too slow at moderate temperatures to be of major concern.^{22,24,25} This conclusion is re-examined here.

Fig. 8 shows typical effluent hydroxyl and silicate compositions from sodium-exchanged Wilmington sand after continuous injection of caustic at 52 ° C. Data are shown at various inlet hydroxide concentrations from our Berkeley laboratory at the U. of California (UCB) and from Petroleum Testing Service (PTS).²⁸ The silicates are reported as parts per million of silicon; they are measured by atomic absorption spectroscopy (AAS) and by spectrophotometry with molybdate complexes. The hydroxide concentrations are determined both by potentiometric titration and by glass electrodes. All compositions refer to ambient temperature. In addition to hydroxide and silicon, the effluent is examined for aluminum and sometimes for iron by AAS. The concentration of these metals, if detected, is always very low; the highest observed is aluminum at approximately 10 ppm. We find that at higher temperatures, higher concentrations of silicates elute. The PTS and UCB data are not comparable directly because differing core lengths and flow rates were used in the two experiments.

Noticeable variations in concentration levels typically are found. These are most likely a result of differences in grain-size distribution and mineralogical composition between and within various core samples. Nevertheless, certain trends always are seen.

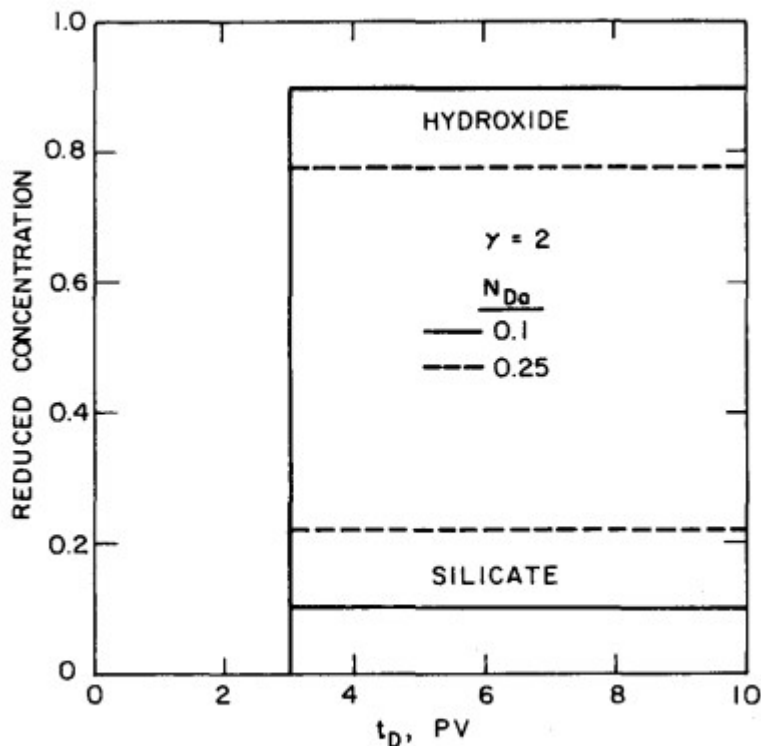


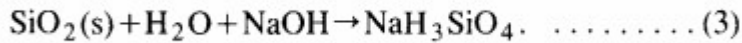
Fig. 9—Predicted hydroxide and silicate concentration histories.

1. Hydroxide elution is delayed—the lower the pH of the injected fluids, the longer the delay. As noted above, the hydroxyl holdup is accounted for by sodium! hydrogen base exchange mainly with reservoir minerals.
2. The hydroxide concentration reaches a constant level but at a concentration slightly below that of the injected fluid.
3. Silicates appear in the core effluent when the alkalinity rises. The silicate level reaches a plateau with its production continuing as long as alkali is injected.

An explanation of these observations follows.

Dissolution of clay minerals, as well as mica and feldspars, should liberate aluminum in significant amounts. Neither aluminum, nor iron, which is commonly associated with clay minerals, is found to any extent in our effluent analyses. The prolonged release of silicates shown in Fig. 8 indicates a source that is present in the core in significant amounts. These observations, when combined with the results of Table 1 and Fig. 1, showing quartz in the fines and whole rock for the Wilmington sands, suggest quartz and amorphous silica as major materials reacting with alkali.

Even in ambient temperature water, silica is effectively infinitely soluble above pH values of about 11.^{23,29} Thus, given long enough, considerable silica in a reservoir will dissolve in alkali. Since only small amounts of silicate are produced in the column tests, we conclude that the alkali-silica reaction is kinetic-controlled. Although the chemistry of soluble silicates is highly complicated,^{23,30} we simplify the dissolution reaction to



Because the silicate concentrations in Fig. 8 are far removed from the solubility limit, we take Reaction 3 as irreversible. For mathematical simplicity, the kinetics are presumed to be first order in hydroxide. Finally, the amount of silica in the core is assumed undepleted during the experiments. Unsteady material balances on hydroxide and silicate (i.e., H_3SiO_4^-) permit prediction of the concentration histories in Fig. 8.

For hydroxide of reduced molar concentration $C_r = C_{\text{OH}}/C_{\text{OH}}^0$ in a water-saturated linear porous medium, we write

$$[1 + \gamma] \frac{\partial C_r}{\partial t_D} + N_{\text{Da}} C_r + \frac{\partial C_r}{\partial x_D} = 0, \dots\dots\dots (4)$$

where $t_D = vt/\phi L$ is the injected PV's of alkali, γ is a reversible ion-exchange delay in equivalent PV's, which in turn is related to the chord of the isotherm in Fig. 6, $x_D = x/L$ is a dimensionless column position, and $N_{\text{Da}} = K_D L/V$ is the Damkohler number for silica dissolution according to Reaction 3-i.e., K_D is a dissolution reaction rate constant, seconds⁻¹. The first term in Eq. 4 corresponds to accumulation in the fluid and on the rock surfaces, the second term indicates loss by Reaction 3, and the third term describes convective transport. For the silicate ions of reduced concentration $C_{\text{rSi}} = C_{\text{Si}}/C_{\text{OH}}^0$ the stoichiometry of Reaction 3 implies that

$$C_{\text{rSi}} = 1 - C_r \dots\dots\dots (5)$$

The solution to Eqs. 4 and 5 is given in Appendix A for continual injection of caustic.

Fig. 9 gives the hydroxide and silicate (i.e., as H_3SiO_4^-) concentration histories from Eqs. 4 and 5 for two different Damkohler numbers. Note that the general features of Fig. 8 are portrayed correctly. The hydroxide is delayed for three PV's by the reversible ion-exchange equilibrium-i.e., γ is set at two. It does not rise to its inlet value because of irreversible loss by reaction with silica. Both silicate and hydroxide reach plateau concentrations because of the large abundance of silica assumed in the core. The most important finding from Fig. 9 is the role of the Damkohler number; higher Damkohler numbers lower the hydroxide and raise the silicate plateau

concentrations. Thus, for long cores and slow flow rates, more consumption of hydroxide is predicted. Some recent experimental evidence supports this contention. * Thus although only small amounts of silicates are produced in laboratory column tests,^{1,22,25} extrapolation by means of the Damkohler number to field well spacings and flooding rates indicates much larger amounts of silica dissolved and alkali consumed. The origin of this effect is the longer residence time of the alkali compared with the characteristic rock-dissolution time in a field application. From Fig. 8 and Eq. A-2 we find provisionally that silica dissolution rate constants, K_D , are between 10^{-7} and 10^{-5} seconds⁻¹ at 52°C. A preliminary discussion is available on the deleterious effects that such dissolution rates have on alkali slugs.²

Conclusions

The following conclusions are based on the work completed and on the specific systems studied.

1. Although the clay mineral contents of the several reservoir oil sands studied were small percentages of the total sand (1 to 2 %), their grain size ($< 2 \mu\text{m}$) and their platy nature make major contributions to the total surface area available for physico-chemical reactions. Other minerals present in the fines and the clay fractions of the oil sands, notably zeolites, also may make substantial contributions to the total reactivity of the sands.
2. Changes in salinity and/or ionic content of fluids flowing through oil sands containing clay-size particles may reduce the flow capacity of the rock significantly.
3. Column tests provide a convenient tool for studying rock/chemical interactions. The technique of frontanalysis chromatography permits accurate determination of equilibrium adsorption isotherms. Because chemical recovery schemes are essentially chromatographic processes, the equilibrium isotherm shapes are as important as the absolute amounts of chemical adsorbed.
4. For Wilmington sands, both sodium/calcium and sodium/hydrogen ion exchange follow mass-action equilibria. Calcium CEC's of California sands reflect their montmorillonite contents.
5. Analysis of effluent species in column testing permits elucidation of any rock/chemical reactions. For Wilmington sands, alkali slowly reacts with silica to produce soluble silicates. Proper scaling of such kinetic-controlled reactions to field conditions is outlined.

Nomenclature

- C = solution concentration, eq/dm³ (eq/L)
 $C_r = C_{OH}/C_{OH}^o$, reduced hydroxide concentration
 $C_{rSi} = C_{Si}/C_{OH}^o$, reduced silicate concentration
 d_{50} = median grain diameter, μm (microns)
 d_{10} = grain size 10% coarser than, μm (microns)
 d_{90} = grain size 90% coarser than, μm (microns)
 k_a = air permeability, md
 k_w = water permeability, md
 K_D = rock dissolution rate constant, seconds⁻¹
 K_I = calcium/sodium, ion-exchange equilibrium constant, dm³/g (L/g)
 L = column length, cm (in.)
 M = mineral-base exchange site
 N = normality, eq/dm³ (eq/L)
 $N_{Da} = K_D L/v$, Damköhler number
 t = time, seconds
 $t_D = vt/\phi L$, PV or reduced time
 v = superficial velocity, m/s (ft/sec)
 x = axial column position, cm (in.)
 $x_D = x/L$, dimensionless axial position
 $Z_{Ca^{++}}$ = calcium ion exchange or adsorption, meq/100 g
 Z_{OH^-} = hydroxide ion exchange or adsorption, meq/100 g
 Z_t = calcium exchange capacity, meq/100 g
 $\gamma = \rho_s \frac{(1-\phi)\Delta Z_{OH^-}}{\phi\Delta C_{OH^-}}$, PV delay of alkali
 ρ_s = solid density, g/cm³
 ϕ = porosity

Superscript

o = inlet

Acknowledgments

This work was performed with financial support from U.S. DOE Contract No. DEAC03-76SF00098 with the Lawrence Berkeley Laboratory, U. of California. We thank Robert Berg and Harold Lechtenberg of the San Francisco office of the U.S. DOE for their encouragement and support. We wish to acknowledge the important roles played by our students: A. Bunge and J. MacGlashan from

chemical engineering; C. Lai, W. Minner, and T. Prescott, petroleum engineering; and A. Jaouni, geology and geophysics.

References

1. Mungan, N.: "Permeability Reduction Through Changes in pH and Salinity," *Trans., AIME* (1965) 234, 1449-53.
2. Radke, C.J. and Somerton, W.H.: "Enhanced Recovery with Mobility and Reactive Tension Agents," paper presented at the 1979 U.S. DOE Symposium on Enhanced Oil and Gas Recovery and Improved Drilling Methods," Tulsa.
3. Hay, R.L.: "Zeolites and Zeolite Reactions in Sedimentary Rocks," GSA Special Paper No. 85 (1966) New York City.
4. Murata, K.J. and Whitely, K.R.: "Zeolites in the Miocene Formations of the Central Coast Ranges, California," *J. Research, USGS* (Feb. 1979) 1, No.3, 255.
5. Muecke, T.W.: "Formation Fines and Factors Controlling Their Movement in Porous Media," *J. Pet. Tech.* (Feb. 1979) 144-50.
6. Wilson, L.A. Jr.: "Physico-Chemical Environment of Petroleum Reservoirs in Relation to Oil Recovery Systems," paper presented at the 1976 AIChE Symposium on Improved Oil Recovery by Surfactant and Polymer Flooding, Kansas City, KS.
7. Smith, F.W.: "Ion-Exchange Conditioning of Sandstones for Chemical Flooding," *J. Pet. Tech.* (June 1978) 959-68.
8. Griffith, T.D.: "Application of Ion-Exchange Processes to Reservoir Preflushes," paper SPE 7587 presented at the 1978 SPE Annual Technical Conference and Exhibition, Houston, Oct. 1-4.
9. Walker, R.D. et al.: "Cation Exchange, Surfactant Precipitation, and Adsorption in Micellar Flooding," ACS Symposium Series 91, R.T. Johansen and R.L. Berg (eds.), ACS, Washington, DC (1979).
10. Hill, H.J. and Lake, L.W.: "Cation Exchange-Chemical Flooding Experiments," paper SPE 6770 presented at the 1977 SPE Annual Technical Conference and Exhibition, Denver, Oct. 9-12.
11. Holm, L.W. and Robertson, S.D.: "Improved Micellar/Polymer Flooding With High-pH Chemicals," *J. Pet. Tech.* (Jan. 1981) 161-72.
12. Campbell, T.E.: "Chemical Flooding: A Comparison Between Alkaline and Soft Preflush Systems," paper SPE 7873 presented at the 1979 SPE Intl. Symposium on Oilfield and Geothermal Chemistry, Houston, Jan. 22-24.
13. Wang, H.L., Duda, J.L., and Radke, E.J.: "Solution Adsorption from Liquid Chromatography," *J. Colloid Int. Sci.* (1978) 66, No.1, 153-65.

14. Shanna, S.C. and Fort, T.: "Adsorption from Solution via Continuous Flow Frontal Analysis Solid-Liquid Chromatography," *J. Colloid Interfacial Sci.* (1973) 43, 36-42.
15. Grimm, R.E.: *Clay Mineralogy*, second edition, McGraw-Hill Book Co. Inc., New York City (1968).
16. Hiester, N.K., Venneulen, T., and Klein, G.: "Adsorption and Ion Exchange," *Perry's Chemical Engineers' Handbook*, fourth edition, J.H. Perry (ed.), McGraw-Hill Book Co. Inc., New York City (1963) Chap. 16.
17. Preston, F.W. and Calhoun, I.C.: "Applications of Chromatography to Petroleum Production Research," *Prod. Monthly* (1952) 16, No.5, 22.
18. Helfferich, F.: *Ion Exchange*, McGraw-Hill Book Co. Inc., New York City (1962).
19. Pope, G.A., Lake, L.W., and Helfferich, F.: "Cation Exchange in Chemical Flooding: Part I-Basic Theory Without Dispersion," *Soc. Pet. Eng. J.* (Dec. 1978) 418-34.
20. Lake, L.W. and Helfferich, F.: "Cation Exchange in Chemical Flooding: Part 2-The Effect of Dispersion, Cation Exchange, and Polymer/Surfactant Adsorption on Chemical Flood," *Soc. Pet. Eng. J.* (Dec. 1978) 435-44.
21. Johnson, C.E. Jr.: "Status of Caustic and Emulsion Methods," *J. Pet. Tech.* (Jan. 1976) 85-92.
22. Ehrlich, R. and Wygal, R.I. Jr.: "Interrelation of Crude Oil and Rock Properties With the Recovery of Oil by Caustic Waterflooding," *Soc. Pet. Eng. J.* (Aug. 1977) 263-70.
23. Stumm, W. and Morgan, J. I.: *Aquatic Chemistry: An Introduction Emphasizing Chemical Equilibria in Natural Waters*, Wiley-Interscience, New York City (1970).
24. Cooke, C.E. Jr., Williams, R.E., and Kolodzie, P.A.: "Oil Recovery by Alkaline Waterflooding," *J. Pet. Tech.* (Dec. 1974) 1365-74.
25. Jennings, H.Y. Jr., Johnson, C.E. Jr., and McAuliffe, C.D.: "A Caustic Waterflooding Process for Heavy Oils," *J. Pet. Tech.* (Dec. 1974) 1334-52.
26. Radke, C.I. and Somerton, W.H.: "Enhanced Recovery With Mobility and Reactive Tension Agents," *Proc., 1978 U.S. ODE Symposium on Enhanced Oil and Gas Recovery and Improved Drilling Methods*, Tulsa, 1, B-2.
27. Bunge, A.L.: "?????", PhD dissertation, U. of California, Berkeley, CA (198).
28. Schweitzer, J. and Schuyler, P.T.: *Petroleum Testing Service Report No. 1292*, prepared for City of Long Beach and THUMS (Oct. 1979).
29. O'Melia, C.R.: "Coagulation and Flocculation," *Physicochemical Processes for Water Quality Control*, W.J. Weber Jr. (ed.), Wiley-Interscience, New York City (1972) Chap. 2.

30. Iler, R.: The Colloid Chemistry of Silica and Silicates. Cornell U. Press, New York City (1955).

Appendix

Hydroxide and Silicate Concentration Histories

Solution to Eqs. 4 and 5 for continual injection of alkali follows. For the hydroxide effluent history we find that

$$C_r(t_D, 1) = \begin{cases} 0, & \text{for } t_D \leq 1 + \gamma \\ \exp(-N_{Da}), & \text{for } t_D \geq 1 + \gamma \end{cases} \quad \dots (A-1)$$

Likewise, for the silicate concentration history we have

$$C_{rSi}(t_D, 1) = \begin{cases} 0, & \text{for } t_D \leq 1 + \gamma \\ 1 - \exp(-N_{Da}), & \text{for } t_D \geq 1 + \gamma \end{cases} \quad \dots (A-2)$$

As noted in the text, Eq. A-2, along with the experimental silicate concentration plateau, permits evaluation of dissolution rate constant, K_D .

SI Metric Conversion Factors

ft	× 3.048*	E-01	= m
°F	(°F-32)/1.8		= °C
in.	× 2.54*	E+00	= cm
microns	× 1.0*	E+00	= μm
mL	× 1.0*	E+00	= cm ³

* Conversion factor is exact.

JPT